

Serial changes in anatomy and ventricular function on dual-source cardiac computed tomography after the Norwood procedure for hypoplastic left heart syndrome

Hyun Woo Goo¹ 

Received: 19 April 2017 / Revised: 4 July 2017 / Accepted: 16 August 2017 / Published online: 6 September 2017
© Springer-Verlag GmbH Germany 2017

Abstract

Background Accurate evaluation of anatomy and ventricular function after the Norwood procedure in hypoplastic left heart syndrome is important for treatment planning and prognostication, but echocardiography and cardiac MRI have limitations.

Objective To assess serial changes in anatomy and ventricular function on dual-source cardiac CT after the Norwood procedure for hypoplastic left heart syndrome.

Materials and methods In 14 consecutive patients with hypoplastic left heart syndrome, end-systolic and end-diastolic phase cardiac dual-source CT was performed before and early (average: 1 month) after the Norwood procedure, and repeated late (median: 4.5 months) after the Norwood procedure in six patients. Ventricular functional parameters and indexed morphological measurements including pulmonary artery size, right ventricular free wall thickness, and ascending aorta size on cardiac CT were compared between different time points. Moreover, morphological features including ventricular septal defect, endocardial fibroelastosis and coronary ventricular communication were evaluated on cardiac CT.

Results Right ventricular function and volumes remained unchanged (indexed end-systolic and end-diastolic volumes: 38.9 ± 14.0 vs. 41.1 ± 21.5 ml/m², $P=0.7$ and 99.5 ± 30.5 vs. 105.1 ± 33.0 ml/m², $P=0.6$; ejection fraction: 60.1 ± 7.3 vs. $63.8 \pm 7.0\%$, $P=0.1$, and indexed stroke volume: 60.7 ± 18.0 vs. 64.0 ± 15.6 ml/m², $P=0.5$) early after the Norwood procedure, but function was decreased (ejection fraction: 64.2 ± 2.6 vs. $58.1 \pm 7.1\%$, $P=0.01$) and volume was increased (indexed end-

systolic and end-diastolic volumes: 39.2 ± 14.9 vs. 68.9 ± 20.6 ml/m², $P<0.003$ and 107.8 ± 36.5 vs. 162.9 ± 36.2 ml/m², $P<0.006$, and indexed stroke volume: 68.6 ± 21.7 vs. 94.0 ± 21.3 ml/m², $P=0.02$) later. Branch pulmonary artery size showed a gradual decrease without asymmetry after the Norwood procedure. Right and left pulmonary artery stenoses were identified in 21.4% (3/14) of the patients. Indexed right ventricular free wall thickness showed a significant increase early after the Norwood procedure (25.5 ± 3.5 vs. 34.8 ± 5.1 mm/m², $P=0.01$) and then a significant decrease late after the Norwood procedure (34.8 ± 5.1 vs. 27.2 ± 4.2 mm/m², $P<0.0001$). The hypoplastic ascending aorta smaller than 2 mm in diameter was identified in 21.4% (3/14) of the patients. Ventricular septal defect ($n=3$), endocardial fibroelastosis ($n=2$) and coronary ventricular communication ($n=1$) were detected on cardiac CT. **Conclusion** Cardiac CT can be used to assess serial changes in anatomy and ventricular function after the Norwood procedure in patients with hypoplastic left heart syndrome.

Keywords Child · Computed tomography · Heart · Hypoplastic left heart syndrome · Norwood procedure · Ventricular function

Introduction

Hypoplastic left heart syndrome is a fatal congenital heart disease in which the underdeveloped left side of the heart fails to support systemic circulation [1]. Therefore, the syndrome is categorized into a functional single ventricle and generally requires three-stage surgical palliation: (1) Norwood operation (in the newborn period; the optimal timing, however, has not been specified yet), (2) bidirectional superior cavopulmonary connection (usually 4–8 months of age), and (3) total cavopulmonary connection (usually between 18 months and

✉ Hyun Woo Goo
ghw68@hanmail.net

¹ Department of Radiology and Research Institute of Radiology, University of Ulsan College of Medicine, Asan Medical Center, 88, Olympic-ro 43-gil, Songpa-gu, Seoul 05505, South Korea

5 years of age). Alternative management includes a hybrid procedure consisting of bilateral pulmonary artery banding and patent ductus arteriosus stenting and bilateral pulmonary artery banding with maintenance of prostaglandin E1 to keep the ductus arteriosus patent. Despite recent improvements in clinical outcomes, the Norwood operation still remains a high-risk surgical procedure requiring careful serial imaging evaluation to maintain adequate systemic, pulmonary and coronary circulations [2]. For that purpose, echocardiography [3], cardiac MRI [4, 5] and cardiac catheterization [2] have been used. However, echocardiography is often limited by operator dependency and obscured acoustic window. In addition, subjective echocardiographic evaluation of right ventricular function in hypoplastic left heart syndrome showed a high discordance rate (>40%) even in the most experienced operators [6]. Cardiac MRI in young children is limited mainly by long examination time and low spatial resolution. Cardiac catheterization may have recently decreased but still non-negligible procedure-related major and minor complication rates especially in newborns and small infants [7]. On the other hand, cardiac catheterization may be performed to check hemodynamic parameters prior to the second and third stages of surgical palliation.

Cardiac CT is a fast diagnostic imaging method useful for evaluating congenital heart disease [8–10]. High spatial resolution of cardiac CT seems to be particularly beneficial for the anatomical evaluation of complex congenital heart disease in young children. On top of that, cardiac CT can provide accurate and reproducible CT volumetry by using high-resolution isotropic three-dimensional (3-D) image data, even for the geometrically complex right ventricle. However, serial changes in anatomy and ventricle function after the Norwood procedure, to the best of my knowledge, have not been evaluated with cardiac CT in hypoplastic left heart syndrome. Therefore, this study aimed to assess serial changes in anatomy and ventricular function on dual-source cardiac CT after the Norwood procedure for hypoplastic left heart syndrome.

Materials and methods

Study population

This retrospective study was approved by the local Institutional Review Board and informed consent was waived. Between December 2013 and July 2016, 14 consecutive patients (M:F=9:5) who underwent cardiac CT examinations to assess the anatomy and ventricular function before and after the Norwood procedures as a first-stage surgical palliation for hypoplastic left heart syndrome were included in this study. The types of hypoplastic left heart syndrome based on echocardiographic results were mitral atresia and aortic atresia ($n=7$), mitral atresia and aortic stenosis ($n=3$), mitral stenosis and aortic stenosis ($n=3$), and a variant ($n=1$) in which the left heart is small without

valvular atresia or stenosis. Bilateral pulmonary artery banding was performed in four high-risk patients with insufficient systemic circulation prior to the Norwood operation and atrial septectomy also was performed in one of the four high-risk patients showing a restrictive left-to-right shunt via a patent foramen ovale. To maintain pulmonary circulation in the Norwood procedure, a right ventricle to pulmonary artery conduit, the Sano modification, was placed in 12 patients and a modified Blalock-Taussig shunt was inserted in two patients. In three patients, the right ventricle to pulmonary artery conduit was partially clipped to facilitate subsequent adjustment of pulmonary blood flow [11]. In one patient with the right ventricle to pulmonary artery conduit, the conduit was replaced by a modified Blalock-Taussig shunt to promote pulmonary artery growth.

Cardiac CT

Electrocardiogram (ECG)-synchronized cardiac CT was performed by using a 128-slice dual-source scanner (SOMATOM Definition Flash; Siemens Healthcare, Forchheim, Germany) with $2 \times 64 \times 0.6$ -mm slices with z-flying focal spot technique, a 0.28-s gantry rotation time, a 75-ms temporal resolution, a 0.75-mm slice width and a 0.4-mm reconstruction interval during free-breathing in all patients. To sedate the patients, oral chloral hydrate (50 mg/kg) was initially used and intravenous midazolam (0.1 mg/kg) or ketamine (1 mg/kg) was additionally administered as required. The patients' heart rate and R-R interval during the cardiac CT scans were 138.9 ± 15.3 (mean \pm standard deviation) beats per minute and 435.4 ± 50.6 ms, respectively. For each cardiac CT examination, both end-systolic and end-diastolic phases were obtained to evaluate ventricular function. As previously described [9], the end-systolic phase was targeted to the second half of the T wave on ECG and a fixed trigger of -35 ms was used to target the end-diastolic phase. When the T wave was not definite or showed an abnormal shape on ECG, a longer acquisition, i.e. 100 ms, was obtained around the estimated end-systolic phase and four data sets were reconstructed by every 25-ms interval to find the most accurate end-systolic phase. Fourteen cardiac CT examinations were performed before the Norwood operation (mean \pm standard deviation, 4.4 ± 3.6 days of age), with 14 cardiac CT examinations acquired within 65 days after the Norwood operation (45.8 ± 14.1 days of age; 30.7 ± 16 days after the Norwood operation), and six cardiac CT examinations obtained immediately before a second-stage surgical palliation (age and postoperative months median: 4.5 months, range: 4–12 months). Prospectively ECG-triggered sequential scan was used in 30 cardiac CT examinations, combined prospectively ECG- and respiratory-triggered sequential scan [12] in 3, and retrospectively ECG-gated spiral scan in 1.

To obtain uniform image noise, a volume CT dose index value based on a 32-cm phantom was individually determined based on the cross-sectional area and mean body density measured on an axial CT image obtained approximately 1–2 cm

above the dome of the liver for bolus tracking [13]. Regarding tube voltage, 70 kV was used in 33 cardiac CT examinations and 80 kV was used in 1. For image reconstruction, the sinogram-affirmed iterative reconstruction (SAFIRE; Siemens Healthcare, Forchheim, Germany) strength 5 with a medium smooth kernel (I26f) was used. Iodinated contrast agent (Iomeron 400, 400 mg I/ml; Bracco Imaging SpA, Milan, Italy; 1.5–2.0 ml/kg) was intravenously administered at an injection rate of 0.2–0.5 ml/s by using a dual-head power injector and a tri-phasic injection protocol, in which undiluted contrast agent was followed by 50% diluted contrast agent and then by 5% diluted contrast agent, to achieve uniform cardiovascular enhancement and minimal peri-venous streak artifacts from undiluted contrast agent. The scan delay time was determined by a bolus tracking technique with a trigger threshold of 150 Hounsfield units (HU) in the left ventricular cavity.

The volume CT dose index and dose-length product values based on a 32-cm phantom of cardiac CT were 2.7 ± 1.6 mGy and 24.2 ± 18.8 mGy-cm, respectively. Effective dose is an estimate of relative whole-body biological risk from a nonuniform partial-body radiation exposure calculated in a reference patient and, therefore, is not applicable to individual patients. Nonetheless, effective dose is widely used in clinical research

and medical communications to weigh the risks and benefits of an imaging study using ionizing radiation. Effective dose values of cardiac CT calculated by multiplying the dose-length product times the age, gender, tube voltage-specific conversion factors for chest CT [14, 15] were 1.5 ± 1.3 mSv.

The quality control of cardiac CT and CT ventricular volumetry and the image interpretation of cardiac CT images were performed by a pediatric radiologist (H.G.W., with 17 years of experience in pediatric cardiac CT). Diagnostic quality of the cardiac CT images was defined when the images showed clear delineation of cardiovascular structures with sufficient cardiovascular enhancement and without substantial motion artifacts.

Semiautomatic 3-D threshold-based ventricular volumetry using cardiac CT data

A stack of thin axial cardiac CT data was sent to a commercially available workstation (Advantage Windows 4.6; GE Healthcare, Milwaukee, WI, USA) for 3-D and multiplanar image evaluation. For CT ventricular volumetry, a 3-D threshold-based segmentation method that enables the exclusion of the papillary muscles and trabeculations from the ventricular cavity was used (Fig. 1). An optimal segmentation threshold

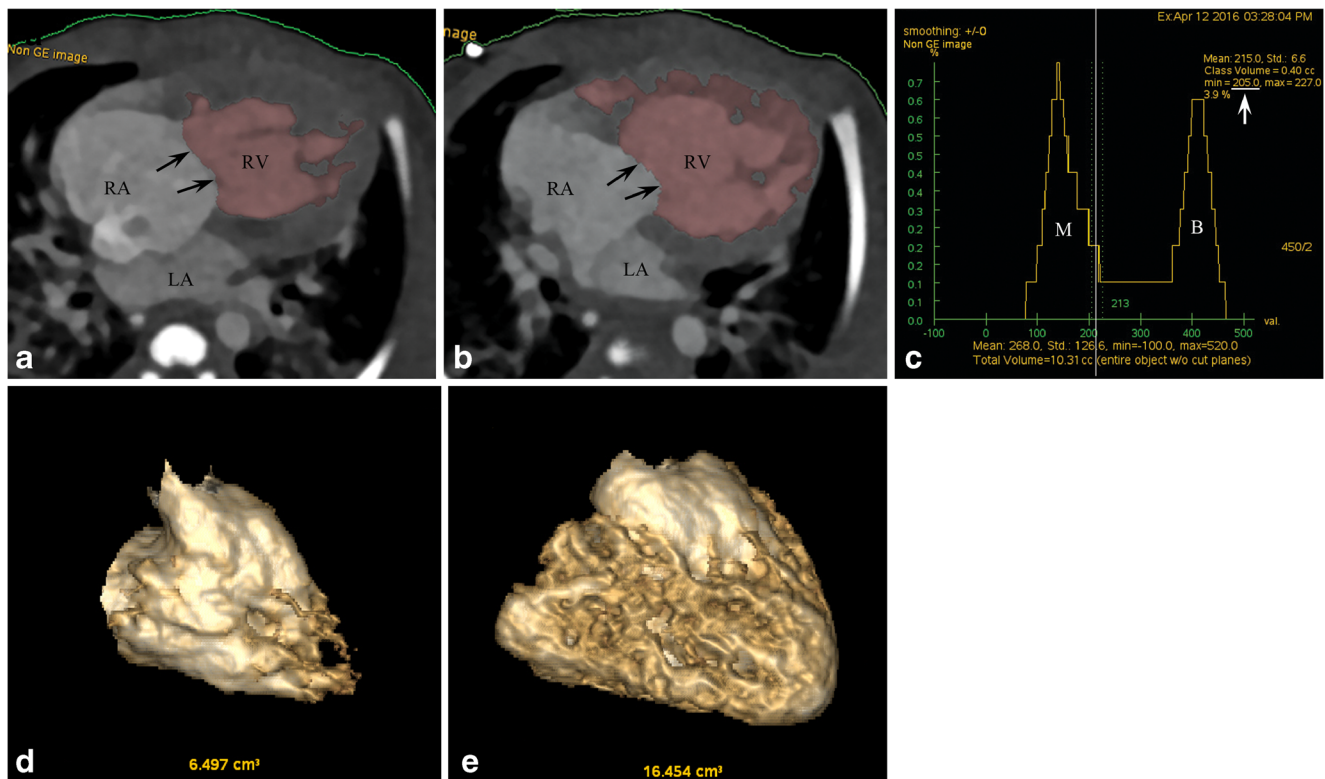


Fig. 1 A 6-day-old female newborn with hypoplastic left heart syndrome (mitral atresia and aortic atresia). End-systolic (a) and end-diastolic (b) four-chamber cardiac CT images show the segmented right ventricular cavity in pink. The papillary muscles and trabeculations of the right ventricle were excluded by using a 3-D threshold-based segmentation method. The tricuspid valve plane (arrows) was manually adjusted. c A histogram

demonstrates two different distribution curves of the myocardium (M) and the ventricular blood (B). Based on the histogram, an optimal threshold (arrow) was determined to be 205 Hounsfield units. End-systolic (d) and end-diastolic (e) volumes of the systemic right ventricle could be calculated by means of the semiautomatic 3-D threshold-based segmentation method. LA left atrium, RA right atrium, RV right ventricle

that separates the most compact myocardium from ventricular blood was selected for each cardiac phase (end-systolic phase: 169.9±26.5 HU, end-diastolic phase: 177.3±24.1 HU) by using a histogram-assisted analysis (Fig. 1) [16, 17]. The atrio-ventricular valve planes were manually adjusted by using a 3-D region-growing editing tool and the semilunar valve planes were manually corrected by using a 3-D scalpel. End-systolic and end-diastolic ventricular volumes calculated for each cardiac CT examination (Fig. 1) were indexed to body surface area. Stroke volume and ejection fraction were subsequently calculated as follows: stroke volume=end-diastolic ventricular volume–end-systolic ventricular volume; ejection fraction (%)=(stroke volume/end-diastolic ventricular volume)×100. The calculated stroke volumes also were indexed to body surface area. Ventricular function of the systemic right ventricle could be assessed in all 14 patients. Ventricular function of the hypoplastic left ventricle was assessable only in seven patients because the hypoplastic left ventricle was not visualized on cardiac CT in the seven remaining patients.

Morphological evaluation on cardiac CT

The diameters of the branch pulmonary artery (anteroposterior diameter+superoinferior diameter/2), ascending aorta and descending aorta at the diaphragm were measured on end-systolic cardiac CT and indexed to body surface area. Right ventricular free wall thickness was measured at the mid-ventricular level on an end-systolic four-chamber cardiac CT image and also indexed to body surface area. Stenosis of the branch pulmonary artery, aortic arch, shunt and conduit was defined when a degree of narrowing in diameter was greater than 50%. The size of the hypoplastic ascending aorta was evaluated when it was smaller than 2 mm in diameter. The presence of ventricular septal defect, left ventricular hypertrophy, endocardial fibroelastosis (endocardial hypodensity on cardiac CT), coronary ventricular communication, coronary artery anomaly and anomalous pulmonary venous return was evaluated. The branching pattern of the aortic arch was evaluated. Moreover, other cardiovascular, airway, lung and other thoracic morphological abnormalities were assessed on cardiac CT.

Statistical analysis

Continuous variables are presented as mean±standard deviation or median with range, and categorical variables are expressed as frequency with percentage. Paired continuous variables measured on cardiac CT were compared between different time points, i.e. before vs. after the Norwood procedure and early vs. late after the Norwood procedure, for each patient using paired *t*-test when the number of the variables for comparison was greater than five. A *P*-value of less than 0.05

was considered to be statistically significant. Statistical analyses were performed using Excel (Microsoft Corporation, Redmond, WA).

Results

In the 14 patients with hypoplastic left heart syndrome, 34 end-systolic and end-diastolic phase cardiac CT examinations were performed with diagnostic quality and without complications.

Ventricular function assessment

Serial changes in CT-based systemic right ventricular functional parameters after the Norwood procedure are described in Tables 1 and 2. No significant differences in the right ventricular functional parameters including indexed end-systolic and end-diastolic volumes (38.9±14.0 vs. 41.1±21.5 ml/m², *P*=0.7; 99.5±30.5 vs. 105.1±33.0 ml/m², *P*=0.6), ejection fraction (60.1±7.3 vs. 63.8±7.0%, *P*=0.1) and indexed stroke volume (60.7±18.0 vs. 64.0±15.6 ml/m², *P*=0.5) were found before and early after the Norwood procedure in all 14 patients (Table 1). In the six patients who underwent cardiac CT late after the Norwood procedure, the systemic right ventricles demonstrated significant increases in indexed end-systolic and end-diastolic volumes (68.9±20.6 vs. 39.2±14.9 or 32.9±8.3 ml/m², *P*<0.02 or 0.003; 162.9±36.2 vs. 107.8±36.5 or 95.0±22.7 ml/m², *P*<0.01 or 0.006) and indexed stroke volume (94.0±21.3 vs. 68.6±21.7 or 62.1±16.7 ml/m², *P*=0.01 or 0.02), and significant reductions in ejection fraction (58.1±7.1 vs. 64.2±2.6 or 65.3±5.7%, *P*=0.07 or 0.01) late after the Norwood procedure, compared with the presurgical or early postsurgical values (Table 2). As in the systemic right ventricles, there were no significant differences in indexed end-systolic and end-diastolic volumes (5.7±2.6 vs. 6.0±4.9 ml/m², *P*=0.8; 10.6±6.0 vs. 12.2±10.9 ml/m², *P*=0.5), ejection fraction (40.8±18.4 vs. 46.1±28.7%, *P*=0.5), and indexed stroke volume (4.8±3.8 vs. 6.1±6.7 ml/m², *P*=0.4) of the hypoplastic left ventricle before and early after the Norwood procedure in the seven patients (Table 3). In the three patients,

Table 1 Changes in systemic right ventricular functional parameters measured by cardiac CT early (1 month) after the Norwood procedure in 14 patients with hypoplastic left heart syndrome

	Pre-Norwood (n=14)	Early post-Norwood (n=14)	<i>P</i> -value
RV ESVi (ml/m ²)	38.9±14.0	41.1±21.5	0.7
RV EDVi (ml/m ²)	99.5±30.5	105.1±33.0	0.6
EF (%)	60.1±7.3	63.8±7.0	0.1
Indexed stroke volume (ml/m ²)	60.7±18.0	64.0±15.6	0.5

EF ejection fraction, *RV EDVi* indexed right ventricular end-diastolic volume, *RV ESVi* indexed right ventricular end-systolic volume

Table 2 Changes in systemic right ventricular functional parameters measured by cardiac CT early (1 month) and late (4.5 months) after the Norwood procedure in 6 patients with hypoplastic left heart syndrome

	Pre-Norwood (n=6)	Early post-Norwood (n=6)	Late post-Norwood (n=6)	P-value*
RV ESVi (ml/m ²)	39.2±14.9	32.9±8.3	68.9±20.6	<0.02, <0.003
RV EDVi (ml/m ²)	107.8±36.5	95.0±22.7	162.9±36.2	<0.01, <0.006
EF (%)	64.2±2.6	65.3±5.7	58.1±7.1	0.07, 0.01
Indexed stroke volume (ml/m ²)	68.6±21.7	62.1±16.7	94.0±21.3	0.01, 0.02

*Two P-values indicate statistical significances of comparisons between pre-Norwood and late post-Norwood groups, and early and late post-Norwood groups, respectively

EF ejection fraction, RV EDVi indexed right ventricular end-diastolic volume, RV ESVi indexed right ventricular end-systolic volume

the ventricular functional parameters of the hypoplastic left ventricles showed serial changes early and late after the Norwood procedure similar to those of the systemic right ventricles, except for the indexed stroke volume: indexed end-systolic volume, 4.4±2.7 vs. 3.2±2.0 vs. 10.2±7.9 ml/m²; indexed end-diastolic volume, 9.6±6.1 vs. 8.9±3.4 vs. 14.8±10.2 ml/m²; ejection fraction, 52.1±9.3 vs. 66.3±16.6 vs. 31.2±14.4%; and indexed stroke volume, 5.2±3.5 vs. 5.6±1.9 vs. 4.7±2.9 ml/m².

Morphological assessment

Serial changes in cardiac CT-based morphological measurements after the Norwood procedure are summarized in Tables 4 and 5. Early after the Norwood procedure, indexed right pulmonary artery and ascending aorta diameters demonstrated significant decreases ($P<0.05$), but indexed right ventricular free wall thickness showed significant increase ($P=0.005$); no significant changes in indexed diameters of the left pulmonary artery

Table 3 Changes in hypoplastic left ventricular functional parameters measured by cardiac CT early (1 month) after the Norwood procedure in 7 patients with hypoplastic left heart syndrome

	Pre-Norwood (n=7)	Early post-Norwood (n=7)	P-value
LV ESVi (ml/m ²)	5.7±2.6	6.0±4.9	0.8
LV EDVi (ml/m ²)	10.6±6.0	12.2±10.9	0.5
EF (%)	40.8±18.4	46.1±28.7	0.5
Indexed stroke volume (ml/m ²)	4.8±3.8	6.1±6.7	0.4

EF ejection fraction, LV EDVi indexed left ventricular end-diastolic volume, LV ESVi indexed left ventricular end-systolic volume

and the descending aorta at the diaphragm ($P>0.05$) as well as tricuspid/mitral valve ratio and indexed tricuspid and mitral valve diameters ($P>0.05$) were found (Table 4).

Indexed right and left pulmonary artery diameters were serially decreased early and late after the Norwood procedure (Table 5). Indexed right ventricular free wall thickness showed a significant increase early after the Norwood procedure (25.5±3.5 vs. 34.8±5.1 mm/m², $P=0.01$) and then a significant decrease late after the Norwood procedure (34.8±5.1 vs. 27.2±4.2 mm/m², $P<0.0001$) (Table 5). Indexed ascending aorta diameter showed small gradual decreases early and late after the Norwood procedure and eventually reached a significant decrease (18.9±7.7 vs. 14.9±6.3 mm/m², $P=0.04$) (Table 5). Indexed diameter of the descending aorta at the diaphragm was statistically unchanged early after the Norwood procedure and then substantially decreased late after the Norwood procedure (28.9±3.0 vs. 21.6±3.0 mm/m², $P=0.02$) (Table 5). Tricuspid/mitral valve ratio was serially increased especially late after the Norwood procedure, probably as a result of a disproportionate decrease between indexed tricuspid and mitral valve annulus diameters (Table 5).

On cardiac CT, right and left pulmonary artery stenoses were identified in 21.4% (3/14) of the patients (Fig. 2). The right ventricle to pulmonary artery conduit showed no stenosis early after the Norwood procedure and stenosis in 16.7% (1/6) of the patients late after the Norwood procedure (Fig. 3). The conduit frequently (66.7%, 4/6) demonstrated mild long-segment narrowing due to pseudointimal hyperplasia late after the Norwood procedure (Fig. 3). The three patients with a modified Blalock-Taussig shunt showed no stenosis. Aortic coarctation (Fig. 4) was initially present in 50% (7/14) of the patients and there was no postsurgical aortic coarctation. The hypoplastic ascending aorta smaller than 2 mm in diameter was identified in 21.4% (3/14) of the patients before the Norwood procedure (Fig. 5). The branching pattern of the aortic arch was normal in all 14 patients. Ventricular septal defect was identified in 21.4% (3/14) of the patients (Fig. 6). Left ventricular hypertrophy was seen in 42.9% (3/7) of the patients with a visible left ventricle (Fig. 7). Endocardial fibroelastosis was detected in 14.3% (2/14) of the patients and the two also showed left ventricular hypertrophy (Fig. 7). Coronary artery anomaly was identified in 14.3% (2/14) of the patients: high takeoff right coronary artery and single coronary artery. Coronary ventricular communication (Fig. 8) was detected in one patient with mitral atresia and aortic stenosis who also had left ventricular hypertrophy and endocardial fibroelastosis.

Additional anatomical findings detected on cardiac CT are summarized in Table 6. Cardiac morphological findings according to the visibility of a hypoplastic left ventricle on cardiac CT are described in Table 7.

Table 4 Changes in cardiac CT-based morphological measurements early (1 month) after the Norwood procedure in hypoplastic left heart syndrome

	Pre-Norwood	Early post-Norwood	P-value
Indexed right pulmonary artery diameter (mm/m ²) (n=10)*	22.8±3.7	17.9±3.0	0.005
Indexed left pulmonary artery diameter (mm/m ²) (n=10)*	22.8±3.9	18.8±5.3	0.06
Indexed right ventricular free wall thickness (mm/m ²) (n=14)	24.5±8.3	32.5±8.2	0.005
Indexed ascending aorta diameter (mm/m ²) (n=14)	18.3±6.8	15.0±5.3	<0.05
Indexed descending aorta diameter at diaphragm (mm/m ²) (n=14)	33.5±4.0	31.6±5.9	0.4
Tricuspid/mitral valve ratio (n=5)†	1.9±0.3	2.2±0.7	0.3
Indexed tricuspid valve annulus diameter (mm/m ²) (n=5)†	52.2±10.2	53.9±12.2	0.7
Indexed mitral valve annulus diameter (mm/m ²) (n=5)†	27.0 ± 3.6	25.0 ± 4.1	0.1

*The measurements could not be obtained in four patients with bilateral pulmonary artery banding

† Of seven patients with visible left ventricle, the mitral valve annulus could not be measured in two patients with a muscular type of mitral atresia

Discussion

This study demonstrated that cardiac CT can be used to assess serial changes in anatomy and ventricular function after the Norwood procedure in patients with hypoplastic left heart syndrome. The serial changes in these imaging parameters are critically important in determining patient management and predicting patient outcome. For example, appropriate medical, interventional and surgical procedures may be planned for patients showing poor systemic right ventricular function or poor pulmonary artery growth due to focal stenosis. Because echocardiography has inherent limitations in providing all necessary data, particularly accurate right ventricular function, pulmonary artery growth and postsurgical aortic coarctation, cardiac CT is essential to provide such valuable information at several time points, e.g., three times in this study (before, early after and late after the Norwood procedure), before the second-stage surgical palliation, i.e.

bidirectional superior cavopulmonary connection, for hypoplastic left heart syndrome. Although cardiac MRI can provide comparable information, cardiac CT is not only widely available but also fast and easy to perform and interpret. Consequently, cardiac CT can be used as an alternative to cardiac MRI for this purpose depending on an institution’s situation and preference.

In this study, systemic right ventricular function and volumes remained almost unchanged approximately 1 month on average after the Norwood procedure in 14 patients with hypoplastic left heart syndrome, but function was decreased and volume was increased around 4.5 months after the Norwood procedure. A previous study using cardiac MRI [4] reported decreased right ventricular function (58.0±8.9% vs. 49.9 ±5.4%, P<0.05) but unchanged indexed end-diastolic right ventricular volumes (102±33 mL/m² vs. 105±33 mL/m², P>0.05) 2.5 months after Sano modification of the Norwood procedure in 20 patients with hypoplastic left heart syndrome.

Table 5 Changes in cardiac CT-based morphological measurements early (1 month) and late (4.5 months) after the Norwood procedure in hypoplastic left heart syndrome

	Pre-Norwood	Early post-Norwood	Late post-Norwood	P-value*
Indexed right pulmonary artery diameter (mm/m ²) (n=4)†	22.6±4.6	18.0±3.1	17.8±2.8	NA
Indexed left pulmonary artery diameter (mm/m ²) (n=4)†	22.5±3.5	19.1±7.2	15.8±4.0	NA
Indexed right ventricular free wall thickness (mm/m ²) (n=6)	25.5±3.5	34.8±5.1	27.2±4.2	0.01, 0.4, <0.0001
Indexed ascending aorta diameter (mm/m ²) (n=6)	18.9±7.7	14.9±6.3	13.8±5.3	0.08, 0.04, 0.6
Indexed descending aorta diameter at diaphragm (mm/m ²) (n=6)	32.6±3.1	28.9±3.0	21.6±3.0	0.1, <0.001, 0.02
Tricuspid/mitral valve ratio (n=2)	1.7±0.3	1.8±0.1	2.3±0.1	NA
Indexed tricuspid valve annulus diameter (mm/m ²) (n=2)§	51.0±18.6	47.8±11.7	48.2±12.6	NA
Indexed mitral valve annulus diameter (mm/m ²) (n=2)§	29.2±5.7	26.4±4.5	21.8±6.8	NA

*Three P-values between pre-Norwood and early post-Norwood, pre-Norwood and late post-Norwood groups, and early and late post-Norwood groups, respectively

† The measurements could not be obtained in four patients with bilateral pulmonary artery banding

§ Of seven patients with visible left ventricle, two serial postoperative cardiac CT examinations were available only in two patients

NA non-applicable

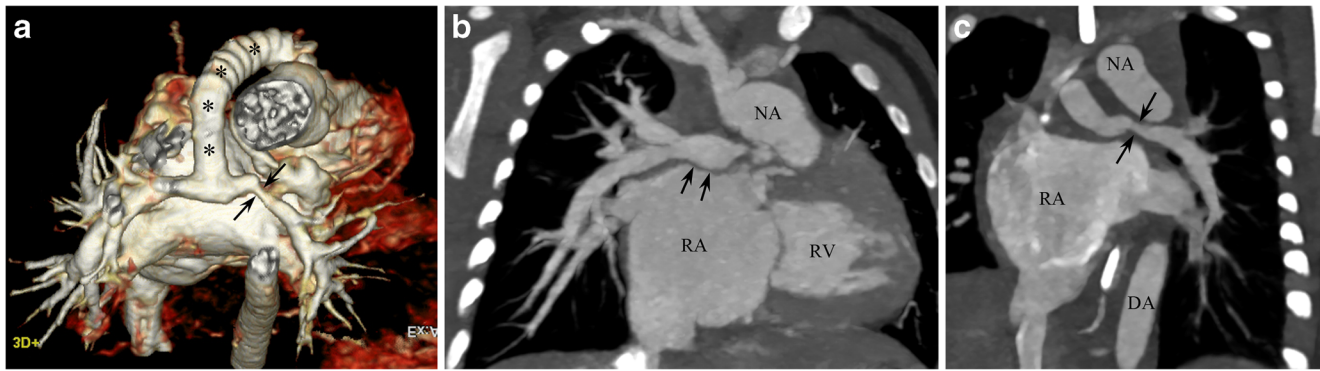


Fig. 2 A 51-day-old boy with hypoplastic left heart syndrome (mitral atresia and aortic atresia) underwent Sano modification of Norwood procedure. **a** Volume-rendered end-systolic cardiac CT image with superior view reveals narrowing (*arrows*) of the left pulmonary artery and the patent right ventricle to pulmonary artery conduit (*asterisks*). Asymmetrically reduced left pulmonary vascularity due to left

pulmonary artery stenosis is noted. **b** Right anterior oblique coronal end-systolic cardiac CT image shows the unobstructed right pulmonary artery (*arrows*). **c** Left pulmonary artery stenosis (*arrows*) also is shown on left anterior oblique coronal end-systolic cardiac CT image. *DA* descending aorta, *NA* neo-ascending aorta, *RA* right atrium, *RV* right ventricle

Based on the results obtained at three different postoperative time points (1, 2.5 and 4.5 months) in the two studies, postoperative changes in ventricular function and volumes likely occur gradually, and a decline in ventricular function may precede an increase in ventricular volumes. These chronological changes help us to determine the most efficient time point of cardiac CT or MRI in these patients. A small difference in the study population from the previous study [4]: Three modified Blalock-Taussig shunts were included in this study. In fact, myocardial damage caused by right ventriculotomy during Sano modification of the Norwood operation is presumed to aggravate regional myocardial dysfunction [18].

In contrast to ventricular function and volumes, serial changes in right ventricular mass, as far as I am aware, have

not been reported after the Norwood procedure in hypoplastic left heart syndrome. In this study, the degree of right ventricular hypertrophy was indirectly quantified by measuring right ventricular free wall thickness on cardiac CT. Of interest, indexed right ventricular free wall thickness was temporarily increased early after Norwood procedure and returned to the presurgical values late after the Norwood procedure. Thus, this early right ventricular hypertrophy may be regarded as a compensatory mechanism to adapt the systemic right ventricle to volume overload and increased afterload, and subsequently failed compensatory mechanism late after the Norwood procedure is deemed to result in decreased hypertrophy and increased dilatation, right ventricular maladaptation [19, 20].

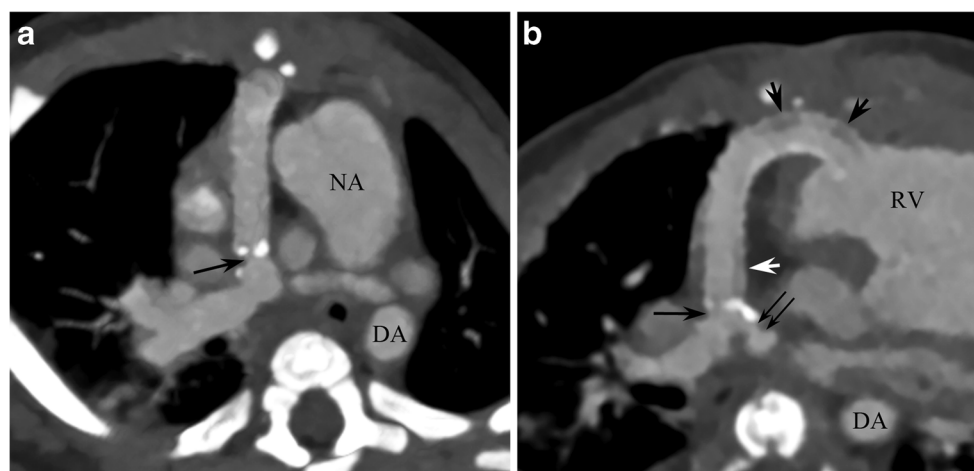


Fig. 3 A 5-month-old girl with hypoplastic left heart syndrome (mitral stenosis and aortic stenosis) underwent Sano modification of the Norwood procedure and bilateral pulmonary artery angioplasty. **a**, **b** Oblique axial end-systolic cardiac CT images show a focal stenosis (*arrow*) of the right ventricle to pulmonary artery conduit. **b** Several

mild long-segment narrowings of the conduit caused by pseudointimal hyperplasia (*short arrows*) and residual left pulmonary artery stenosis (*long arrows*) are noted. *DA* descending aorta, *NA* neo-ascending aorta, *RV* right ventricle

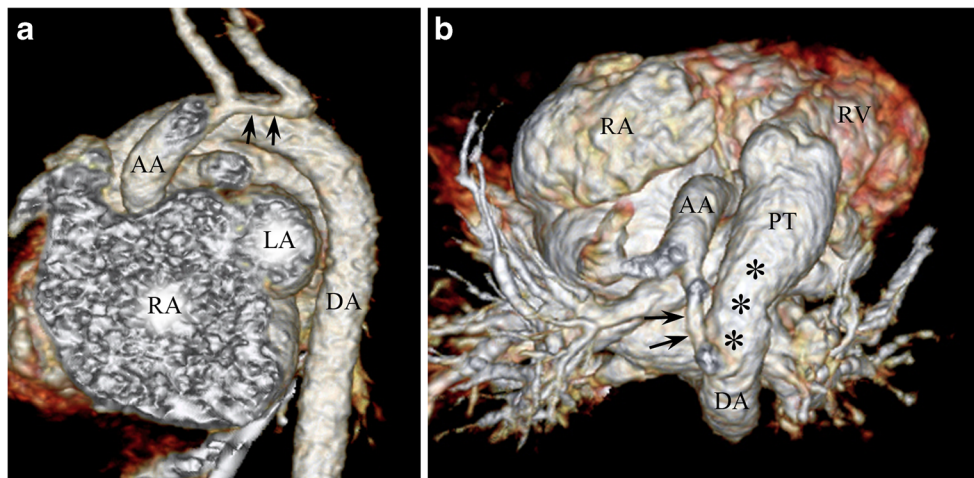


Fig. 4 A 4-day-old male newborn with hypoplastic left heart syndrome (mitral atresia and aortic stenosis). Left lateral (a) and superior (b) volume-rendered end-systolic cardiac CT images show coarctation of the aorta (arrows). The diameters of the ascending aorta, aortic arch and descending aorta at the

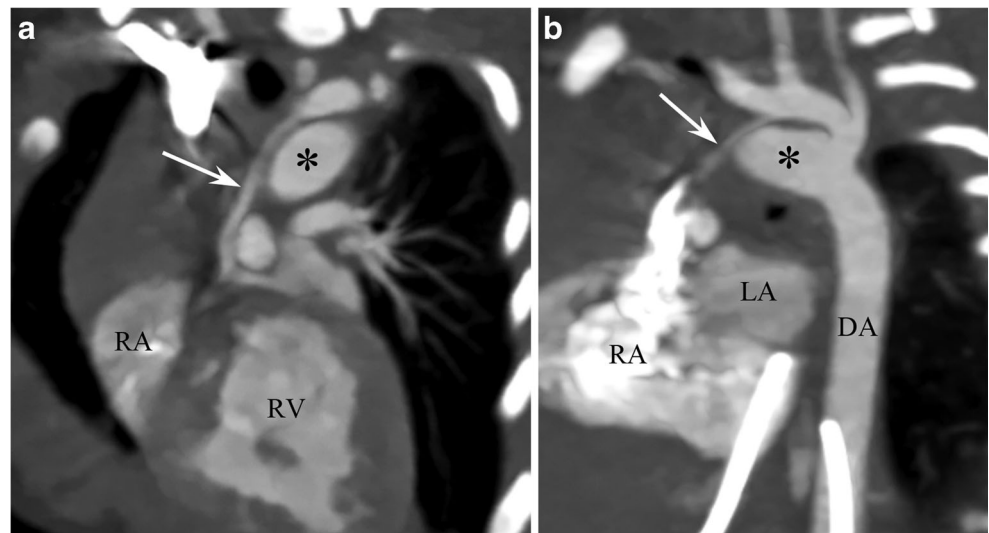
diaphragm measured on cardiac CT were 6.7 mm, 1.6 mm and 8.5 mm, respectively. Large patent ductus arteriosus (asterisks) is noted. AA ascending aorta, DA descending aorta, LA left atrium, PT pulmonary trunk, RA right atrium, RV right ventricle

In addition, hypoplastic left ventricular function and volume could be evaluated and showed similar chronological changes to those of the systemic right ventricle except for stroke volume in this study. The indexed end-diastolic left ventricular volumes ranged widely from 3.3 ml/m² to 36.3 ml/m². Although other parameters, such as mitral valve area and aortic root size, should be considered in determining the feasibility of biventricular repair, a left ventricular end-diastolic volume of 20 ml/m² is often used as one of the key parameters [21]. However, the volume threshold is derived from echocardiographic measurements in critical aortic valve stenosis and echocardiography, compared with cardiac MRI, underestimates a small left ventricular volume [22]. Recently, cardiac CT can provide accurate volume measurement for a small left ventricle [23]. It is plausible that a higher spatial

resolution of cardiac CT than cardiac MRI would be beneficial for volumetry accuracy in small ventricles. In hypoplastic left heart syndrome, a larger left ventricular volume common in the mitral stenosis and aortic atresia subgroup actually results in lower survival because it acts like a space-occupying mass [24]. Furthermore, the septal convexity toward the right ventricle in the mitral stenosis and aortic atresia subgroup, compared with the concave-shaped septum in the mitral atresia and aortic atresia subgroup, may mechanically affect the effective output of the systemic right ventricle [24].

In this study, left ventricular morphological features important in prognosticating hypoplastic left heart syndrome including left ventricular hypertrophy, endocardial fibroelastosis, coronary ventricular communication and ventricular septal

Fig. 5 A 1-day-old female newborn with hypoplastic left heart syndrome (mitral atresia and aortic atresia). Oblique sagittal (a) and oblique coronal (b) end-systolic cardiac CT images demonstrate the 1.8-mm hypoplastic ascending aorta (arrows). The aortic arch was 4.0 mm in diameter without the evidence of aortic coarctation. Large patent ductus arteriosus (asterisks) is noted. DA descending aorta, LA left atrium, RA right atrium, RV right ventricle



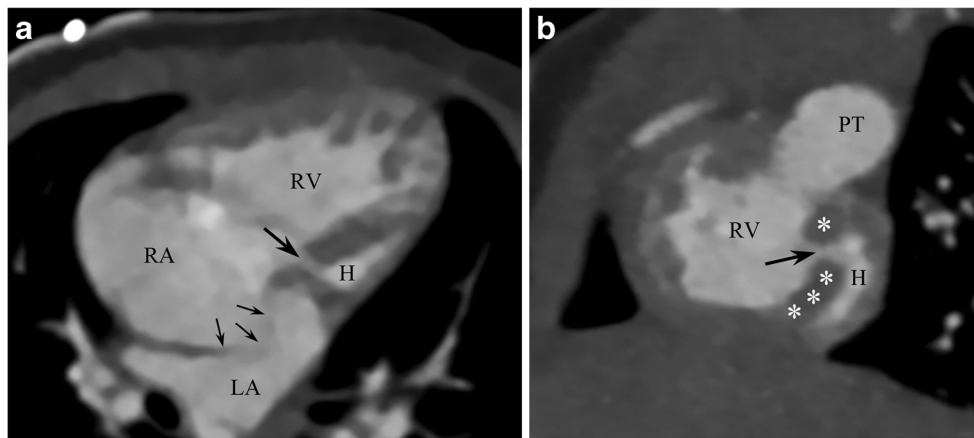


Fig. 6 A 2-day-old female newborn with hypoplastic left heart syndrome (mitral atresia and aortic atresia). End-systolic four-chamber (**a**) and short-axis (**b**) cardiac CT images reveal a small ventricular septal defect (*thick arrow*). The interatrial septum (*thin arrows*) and interventricular septum (*asterisks*) are convex toward the left atrium and the hypoplastic

left ventricle (H), respectively. The cardiac apex is formed by the enlarged right ventricle but not by the hypoplastic left ventricle on four-chamber cardiac CT image (**a**). *DA* descending aorta, *LA* left atrium, *PT* pulmonary trunk, *RA* right atrium, *RV* right ventricle

defect were detected on cardiac CT. It is worth mentioning that ventricular septal defect or coronary ventricular communication might be attributed to enlarge left ventricular cavity in three patients.

In addition to systemic right ventricular function, adequate pulmonary artery growth is critical for long-term clinical outcomes. In this study, indexed branch pulmonary artery diameter demonstrated a gradual decrease after the Norwood procedure on cardiac CT, which is in line with the results of the previous study using cardiac MRI [4]. Greater left pulmonary artery growth was reported in Sano modification of the Norwood procedure [4], which is the opposite of the standard Norwood operation using the right-side modified Blalock-Taussig shunt, leading to greater right pulmonary artery growth. Such

asymmetrical pulmonary artery growth was not evident in this study. Branch pulmonary artery stenosis also was equally detected on both sides in this study. Smaller pulmonary artery size on catheter angiography before the second-stage palliation was reported in the right ventricle to pulmonary artery conduit group than in the modified Blalock-Taussig shunt group [25]. To maintain adequate pulmonary blood flow, the conduit or shunt patency is also important and focal conduit stenosis was detected on cardiac CT in one patient late after the Norwood procedure in this study.

Other morphological features could be evaluated on cardiac CT. Among them, the measurement of the hypoplastic ascending aorta diameter is crucial because a smaller diameter (<2 mm) is associated with increased mortality during the Norwood

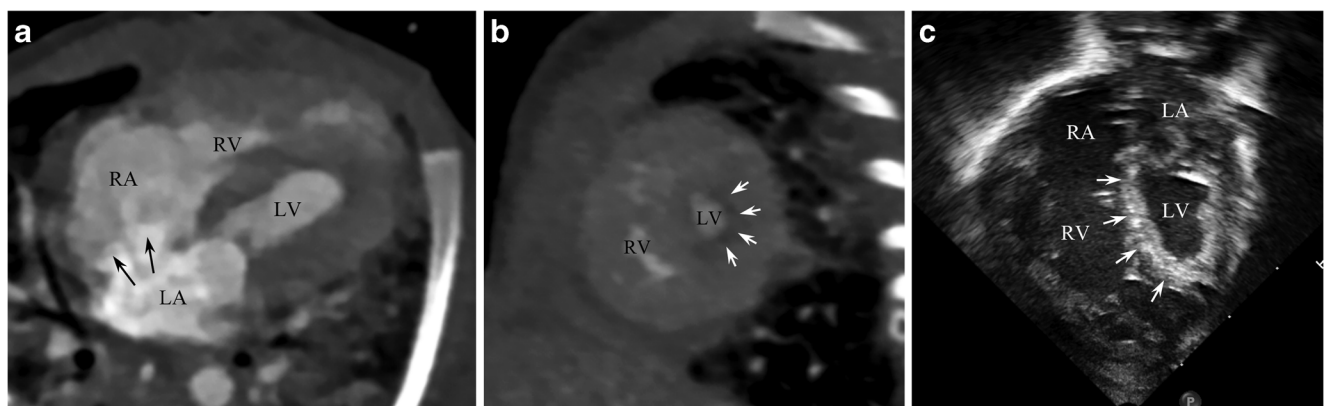


Fig. 7 A 47-day-old boy with hypoplastic left heart syndrome (mitral stenosis and aortic stenosis) underwent Sano modification of the Norwood procedure. End-systolic four-chamber (**a**) and short-axis (**b**) cardiac CT images show left ventricular hypertrophy. A contrast jet (*arrows*) from the left atrium to the right atrium indicating a substantial left-to-right shunt is shown on four-chamber cardiac CT image (**a**). Diffuse left ventricular endocardial hypodensity (*arrows*) suggesting

endocardial fibroelastosis is clearly depicted on short-axis cardiac CT image (**b**), which corresponds with the diffusely echogenic endocardium (*arrows*) of the left ventricle on the apical four-chamber echocardiographic image (**c**). The cardiac apex is formed by the enlarged right ventricle but not by the hypoplastic left ventricle on four-chamber cardiac CT and echocardiographic images (**a**, **c**). *LA* left atrium, *LV* left ventricle, *RA* right atrium, *RV* right ventricle

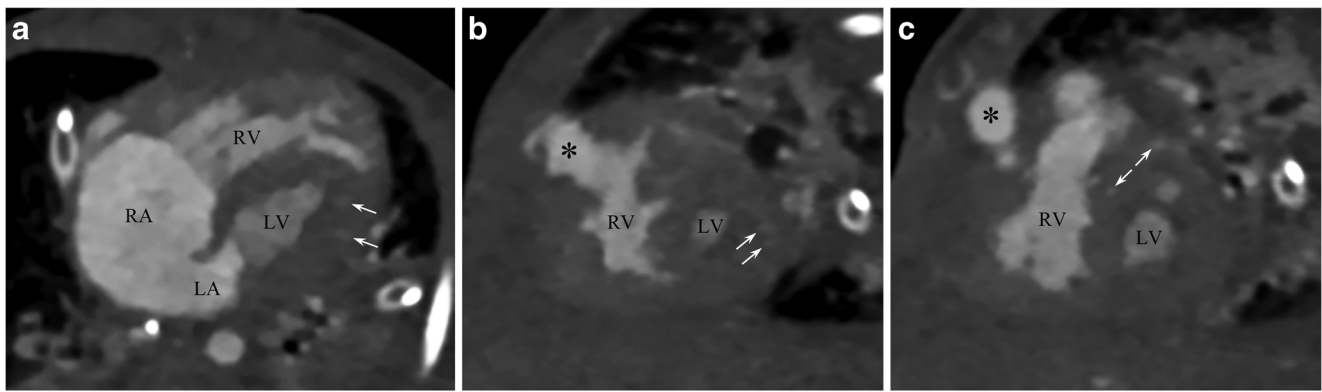


Fig. 8 A 43-day-old boy with hypoplastic left heart syndrome (mitral atresia and aortic stenosis) underwent Sano modification of the Norwood procedure. End-systolic four-chamber (a) and short-axis (b, c) cardiac CT images show multiple enhancing lesions (arrows) in the hypertrophied left ventricular myocardium suggesting coronary ventricular communications that seem to be the main source of left ventricular

filling. In addition, left ventricular endocardial hypodense lesions suggest endocardial fibroelastosis. The cardiac apex is formed by the enlarged right ventricle but not by the hypoplastic left ventricle on four-chamber cardiac CT image (a). LA left atrium, LV left ventricle, RA right atrium, RV right ventricle, * right ventricle to pulmonary artery conduit

operation [2]. Cardiac CT would be advantageous in the diagnostic task because the size of the hypoplastic ascending aorta is so small in newborns and cardiac CT with higher spatial resolution is regarded as superior to cardiac MRI in evaluating neonatal coronary arteries generally smaller than 2 mm in diameter [26]. Coronary artery anatomy is usually normal in hypoplastic left heart syndrome [2], but the incidence of coronary artery anomalies, such as high takeoff right coronary artery and single coronary artery, was unexpectedly high (14.3%) in this study. As described in the literature [2, 27], anomalous pulmonary venous return and airway anomaly was rarely (7.1%) detected in this study. Of note, the former may complicate the surgical approach in the Norwood procedure [2].

Cardiac CT has the potential to offer high-resolution patient-specific anatomical data to help further refine the Norwood procedure individually by using engineering tools [28]. In a case with hypoplastic left heart syndrome palliated with Sano modification of the Norwood procedure, complex

cardiovascular anatomy derived from CT datasets was used for computational fluid dynamics [29].

This study has several limitations. Firstly, the small number of the study population might affect the results of this study including statistical significance. However, hypoplastic left heart syndrome is a rare congenital heart disease and it, therefore, is more difficult to collect a large number of data than other common diseases. Secondly, there might be a selection bias in performing cardiac CT due to a retrospective nature of this study. Nevertheless, the potential use of cardiac CT for evaluating serial changes after the Norwood procedure could be demonstrated in this study. Thirdly, cardiac CT has potential risks associated with ionizing radiation and contrast nephrotoxicity. In this study, radiation dose of cardiac CT was minimized by using various radiation dose-lowering techniques and cardiac CT was performed in patients with normal renal function. Lastly, the temporal resolution of cardiac CT used in this study was lower than those of echocardiography and cardiac MRI, which might affect the accuracy of CT ventricular volumetry.

Table 6 Additional anatomical findings detected on cardiac CT

Additional anatomical findings	Frequency
Bronchial narrowings (mainly compressed by the enlarged heart)	57.1% (8/14)
Bilateral superior vena cava	14.3% (2/14)
Left lower pulmonary vein narrowing	14.3% (2/14)
Partial anomalous pulmonary venous return (the left upper pulmonary vein anomalously draining into the coronary sinus)	7.1% (1/14)
Airway anomaly (right tracheal bronchus)	7.1% (1/14)
Lung anomaly (a small right lung with the dextroposed heart)	7.1% (1/14)
Diffuse body wall swelling	7.1% (1/14)
Dilated inferior vena cava, hepatic veins and internal mammary arteries	7.1% (1/14)

Table 7 Cardiac morphological findings according to the visibility of a hypoplastic left ventricle

No visible left ventricle (n=7)	Visible left ventricle (n=7)
Mitral atresia and aortic atresia, 6	Mitral stenosis and aortic stenosis, 3
Mitral atresia and aortic stenosis, 1	Mitral atresia and aortic stenosis with ventricular septal defect or coronary ventricular communication, 2
	Hypoplastic left heart syndrome variant, 1
	Mitral atresia and aortic atresia with ventricular septal defect, 1

Conclusion

Cardiac CT can be used to assess serial changes in anatomy and ventricular function after the Norwood procedure in patients with hypoplastic left heart syndrome. In this study, cardiac CT could evaluate serial changes in right and left ventricular volumes and functions, and pulmonary artery size after the Norwood procedure. Moreover, cardiac CT could assess the size of hypoplastic ascending aorta, the presence of ventricular septal defect and coronary ventricular communication in these patients. The anatomical and ventricular functional findings identified with cardiac CT are crucial for clinical prognostication.

Compliance with ethical standards

Conflicts of interest None

References

- Barron DJ, Kilby MD, Davies B et al (2009) Hypoplastic left heart syndrome. *Lancet* 374:551–564
- Fonseca BM (2013) Perioperative imaging in hypoplastic left heart syndrome. *Semin Cardiothorac Vasc Anesth* 17:117–127
- Khoo NS, Smallhorn JF, Kaneko S et al (2011) Novel insights into RV adaptation and function in hypoplastic left heart syndrome between the first 2 stages of surgical palliation. *JACC Cardiovasc Imaging* 4:128–137
- Lim DS, Peeler BB, Matherne GP et al (2008) Cardiovascular magnetic resonance of pulmonary artery growth and ventricular function after Norwood procedure with Sano modification. *J Cardiovasc Magn Reson* 10:34
- Bellsham-Revell HR, Tibby SM, Bell AJ et al (2013) Serial magnetic resonance imaging in hypoplastic left heart syndrome gives valuable insight into ventricular and vascular adaptation. *J Am Coll Cardiol* 61:561–570
- Bellsham-Revell HR, Simpson JM, Miller OI et al (2013) Subjective evaluation of right ventricular systolic function in hypoplastic left heart syndrome: how accurate is it? *J Am Soc Echocardiogr* 26:52–56
- Rhodes JF, Asnes JD, Blaurock AD et al (2000) Impact of low body weight on frequency of pediatric cardiac catheterization complications. *Am J Cardiol* 86:1275–1278
- Goo HW (2010) State-of-the-art CT imaging techniques for congenital heart disease. *Korean J Radiol* 11:4–18
- Goo HW (2011) Cardiac MDCT in children: CT technology overview and interpretation. *Radiol Clin N Am* 49:997–1010
- Goo HW (2013) Current trends in cardiac CT in children. *Acta Radiol* 54:1055–1062
- Bradley SM, Erdem CC, Hsia TY et al (2008) Right ventricle-to-pulmonary artery shunt: alternative palliation in infants with inadequate pulmonary blood flow prior to two-ventricle repair. *Ann Thorac Surg* 86:183–188
- Goo HW, Allmendinger T (2017) Combined ECG- and respiratory-triggered CT of the lung to reduce respiratory misregistration artifacts between imaging slabs in free-breathing children: initial experience. *Korean J Radiol* 18:860–866. <https://doi.org/10.3348/kjr.2017.18.5.860>
- Goo HW (2011) Individualized volume CT dose index determined by cross-sectional area and mean density of the body to achieve uniform image noise of contrast-enhanced pediatric chest CT obtained at variable kV levels and with combined tube current modulation. *Pediatr Radiol* 41:839–847
- Deak PD, Smal Y, Kalender WA (2010) Multisection CT protocols: sex- and age-specific conversion factors used to determine effective dose from dose-length product. *Radiology* 257:158–166
- Goo HW (2012) CT radiation dose optimization and estimation: an update for radiologists. *Korean J Radiol* 13:1–11
- Koch K, Oellig F, Oberholzer K et al (2005) Assessment of right ventricular function by 16-detector-row CT: comparison with magnetic resonance imaging. *Eur Radiol* 15:312–318
- Goo HW, Park S (2015) Semiautomatic three-dimensional CT ventricular volumetry in patients with congenital heart disease: agreement between two methods with different user interaction. *Int J Cardiovasc Imaging* 31:223–232
- Menon SC, Minich LL, Casper TC et al (2011) Regional myocardial dysfunction following Norwood with right ventricle to pulmonary artery conduit in patients with hypoplastic left heart syndrome. *J Am Soc Echocardiogr* 24:826–833
- Geva T (2011) Repaired tetralogy of Fallot: the roles of cardiovascular magnetic resonance in evaluating pathophysiology and for pulmonary valve replacement decision support. *J Cardiovasc Magn Reson* 13:9
- Rich S (2012) Right ventricular adaptation and maladaptation in chronic pulmonary arterial hypertension. *Cardiol Clin* 30:257–269
- Kaplinski M, Cohen MS (2015) Characterising adequacy or inadequacy of the borderline left ventricle: what tools can we use? *Cardiol Young* 25:1482–1488
- Grosse-Wortmann L, Yun TJ, Al-Radi O et al (2008) Borderline hypoplasia of the left ventricle in neonates: insights for decision-making from functional assessment with magnetic resonance imaging. *J Thorac Cardiovasc Surg* 136:1429–1436
- Kim HJ, Goo HW, Park SH et al (2013) Left ventricle volume measured by cardiac CT in an infant with a small left ventricle: a new and accurate method in determining uni- or biventricular repair. *Pediatr Radiol* 43:243–246
- Shuhaiber JH, Pigula FA (2013) Left ventricle after palliation of hypoplastic left heart syndrome: friend, fiend, or innocent bystander? *Pediatr Cardiol* 34:1063–1072
- Arnold RR, Loukanov T, Gorenflo M (2014) Hypoplastic left heart syndrome - unresolved issues. *Front Pediatr* 2:125
- Goo HW, Yang DH (2010) Coronary artery visibility in free-breathing young children with congenital heart disease on cardiac 64-slice CT: dual-source ECG-triggered sequential scan vs. single-source non-ECG-synchronized spiral scan. *Pediatr Radiol* 40:1670–1680
- Noel CV, Kovalchin JP, Adler B et al (2014) Incidence of tracheobronchial anomalies found with hypoplastic left heart syndrome. *Congenit Heart Dis* 9:294–299
- Biglino G, Giardini A, Hsia TY et al (2013) Modeling single ventricle physiology: review of engineering tools to study first stage palliation of hypoplastic left heart syndrome. *Front Pediatr* 1:31
- Qian Y, Liu L, Itatani K et al (2010) Computational hemodynamic analysis in congenital heart disease: simulation of the Norwood procedure. *Ann Biomed Eng* 38:2302–2313